processes

MDPI

Article

Proteomics Analysis of *Zygosaccharomyces mellis* in Response to Sugar Stress

Xiaolan Xu [1,2,*,†], Yuxuan Zhu [2,3,†], Yujie Li [2,3], Wenchao Yang [1,2], Hao Zhou [2,3] and Xinchao Chen [2,3]

1 College of Animal Science (College of Bee Science), Fujian Agriculture and Forestry University, Fuzhou 350002, China; beesyang@gmail.com
2 State and Local Joint Engineering Laboratory of Natural Biotoxins, Fuzhou 350002, China; yuxuan18350993003@126.com (Y.Z.); 8105041302@163.com (Y.L.); zhouchuanhao123@gmail.com (H.Z.); chenxinchao2022@163.com (X.C.)
3 College of Food science, Fujian Agriculture and Forestry University, Fuzhou 350002, China
* Correspondence: xlxufz@126.com
† These authors contributed equally to this work.

Abstract: The high-osmotic-pressure environment of honey is not suitable for the survival of microorganisms, except for osmotic-tolerant fungal and bacterial spores. In this study, shotgun metagenomic sequencing technology was used to identify yeast species present in honey samples. As a result, *Zygosaccharomyces* spp. yeast, including *Zygosaccharomyces rouxii*, *Z. mellis* and *Z. siamensis*, were isolated. The intracellular trehalose and glycerin concentrations of yeast, as well as the antioxidant-related CAT, SOD and POD enzyme activities, increased under a high-glucose environment (60%, *w*/*v*). To learn more about the osmotic resistance of *Z. mellis*, iTRAQ-based proteomic technology was used to investigate the related molecular mechanism at the protein level, yielding 522 differentially expressed proteins, of which 303 (58.05%) were upregulated and 219 (41.95%) were downregulated. The iTRAQ data showed that the proteins involved in the pathway of the cell membrane and cell-wall synthesis, as well as those related to trehalose and glycerin degradation, were all downregulated, while the proteins in the respiratory chain and TCA cycle were upregulated. In addition, formate dehydrogenase 1 (FDH1), which is involved in NADH generation, displayed a great difference in response to a high-sugar environment. Furthermore, the engineered *Saccharomyces cerevisiae* strains BY4741△scFDH1 with a knocked-out *FDH*1 gene were constructed using the CRISPR/Cas9 method. In addition, the *FDH*1 from *Z. mellis* was expressed in BY4741△scFDH1 to construct the mutant strain BY4717zmFDH1. The CAT, SOD and POD enzyme activities, as well as the content of trehalose, glycerin, ATP and NADH, were decreased in BY4741△scFDH1. However, those were all increased in BY4717zmFDH1. This study revealed that *Z. mellis* could increase the contents of trehalose and glycerin and promote energy metabolism to improve hypertonic tolerance. In addition, FDH1 had a significant effect on yeast hypertonic tolerance.

Keywords: yeasts; iTRAQ; *Zygosaccharomyces mellis*; *FDH1*; CRISPR/Cas9

Citation: Xu, X.; Zhu, Y.; Li, Y.; Yang, W.; Zhou, H.; Chen, X. Proteomics Analysis of *Zygosaccharomyces mellis* in Response to Sugar Stress. *Processes* **2022**, *10*, 1193. https://doi.org/10.3390/pr10061193

Received: 2 April 2022
Accepted: 10 June 2022
Published: 15 June 2022

1. Introduction

Honey is a natural and stable sweetener that is primarily composed of sugars (70–85%), including fructose, sucrose, glucose, maltose, raffinose and others [1]. Due to high osmotic stress, most microbes cannot survive in honey, except osmotolerant and halotolerant microorganisms, such as yeast *Zygosaccharomyces* spp., which can cause food spoilage. These yeasts are found in a wide range of sugary foods, including fruit juices, wine and honey [2], leading to economic losses in food manufacture and health hazard. Among these species, *Z. rouxii* has been extensively studied for its osmotic tolerance in food fermentation under high sugar or high salt stress. Another yeast isolated from honey, *Z. mellis*, also has remarkably high sugar tolerance [3]. Exploring the molecular mechanisms of resistance under high sugar stress is helpful for developing strategies for food production. Although

previous studies have reported the isolation and identification of *Z. mellis* and the effect of a high-glucose environment on the transcription expression profile, there is *a* lack of in-depth studies on its hypertonic resistance [4–6]. iTRAQ-based proteomic technology could screen differentially expressed proteins (DEPs) that are involved in cell biological processes and help us to better understand the hypertonic mechanism of *Z. mellis*.

The metabolic pathways and response mechanisms of yeasts, especially *Z. rouxii* and *Saccharomyces cerevisiae*, under high osmotic conditions have been widely reported [7–9]. The content of major metabolites in the stress response in yeast, including glycerin, trehalose, D-arabinol and erythritol, is increased under the stress of high concentrations of sugar, NaCl and ethanol [7,10]. At the same time, cells can adapt to stress by regulating the activity of superoxide dismutase (SOD), intracellular peroxidase, adenosine triphosphatase (ATPase) and mitochondrial ATPase [11]. In addition, the high osmolarity glycerol mitogen-activated protein kinase (HOG- MAPK) pathway, which plays a crucial role in signal transduction in yeast, can promote glycerin accumulation and regulate other physiological processes [12,13].

With the development of genomics, proteomics and other molecular technologies, the tolerance mechanisms of yeast can also be studied from a comprehensive perspective at the protein level. For example, in *Z. rouxii*, the proteins involved in carbohydrate and energy metabolism, amino acid metabolism, response to stimulus, etc., were shown to be regulated in response to high sugar concentrations [14]. Unlike *Z. rouxii*, under stationary-phase stress conditions, the cell replication, oxidative stress responses and proteolytic activity of *S. cerevisiae* were decreased, whereas cell-wall renewal, the regulation of solute transport across the cell membrane and de novo arginine synthesis were enhanced [15]. The metabolic processes of *Z. rouxii* and *S. cerevisiae* have been well reported; however, there was few reports on the mechanism of osmo-tolerance in *Z. mellis*. Due to the different and extremely complex metabolic processes, the mechanisms of other yeasts adapted to high-sugar environments need to be further studied.

DNA metabarcoding is a high-throughput molecular identification approach for identifying mixed samples from plants, animals or fungi [16,17]. In this study, the yeasts isolated from honey were identified by DNA barcoding and metabarcoding. Furthermore, the mechanism associated with the sugar tolerance of *Z. mellis* was investigated by proteomic techniques. The findings contribute to a better understanding of the high sugar tolerance features of *Z. mellis*.

2. Materials and Methods

2.1. Isolation and Identification of Honey Samples

A total of 39 honey samples were collected from apiaries in different areas in China (Table S1). The yeasts in each honey sample were identified by the DNA metabarcoding technique [18]. Firstly, the honey was diluted with sterile water and centrifuged at 9000 rpm for 10 min at 4 °C. Then, the total genomic DNA of yeasts from each sample was extracted using TIANamp Yeast DNA Kit (TIANGEN Biotech Co., Ltd., Beijing, China). The primers ITS1 and ITS2 (Table 1) were used for PCR amplification, which was carried out with Phusion® High-Fidelity PCR Master Mix (NEB, Ipswich, MA, USA). The mixed PCR products were purified with a GeneJET Gel Extraction Kit (Thermo Fisher Scientific, San Jose, CA, USA). Sequencing libraries were generated using the Next®Ultra™ DNA Library Prep Kit (NEB, Ipswich, Massachusetts, USA), including the processes of input-DNA fragmentation, end repair, 5′ phosphorylation and dA-Tailing, adaptor ligation, U excision, magnetic-beads purification and PCR enrichment. Finally, the library was sequenced on an Illumina MiSeq platform (Illumina, San Diego, CA, USA). Paired-end reads from the original DNA fragments were merged using FLASH (fast length adjustment of short reads) software to produce longer reads [19]. At last, paired-end reads were assigned to each sample according to the unique barcodes.

Table 1. Primers used in this study.

Name	Sequences 5′ to 3′
ITS1	TCCGTAGGTGAACCTGCGG
ITS2	GCTGCGTTCTTCATCGATGC
FDH1-UP-F	ATAGGCTTGAAAGAGAGTTTTAA
FDH1-UP-R	AATACTCATAATCACTCATTAATTTTCAGCTGTTATTTTG
FDH1-down-F	ATAACAGCTGAAAATTAATGAGTGATTATGAGTATTTGTGAGCA
FDH1-down-R	TTTTCTGCAGCAGATACTTTTGG
scFDH1-KpnI-F	GGGGTACCAACACAATGTCGAAGGGAAAGGTTTTGC
scFDH1-BamHI-R	CGGGATCCTTATTTCTTCTGTCCATAAGCTC
zmFDH1-KpnI-F	GGGGTACCAACACAATGTGCAAGGGCAAGGTGTC
zmFDH1-BamHI-R	CGGGATCCATGGTCAGAAAACAAACTAG
M13-F	CCCAGTCACGACGTTGTAAAACG
M13-R	AGCGGATAACAATTTCACACAGG
T7	TAATACGACTCACTATAGGG
CYC1 Terminator	GTGACATAACTAATTACATGATG
FDH1-F	TTGCTGGCCTCGTTCAATCT
FDH1-R	CCGGCGTGGCTAAAAATGAG

Furthermore, the isolated yeasts were cultured on yeast extract–peptone–dextrose (YPD) agar plates at 30 °C for 2 days. In addition, the amount of yeast was counted according to the method described in "National food safety standard—honey" in China (GB 14963-2011). Then, the single yeast colony was selected and incubated in YPD medium at 30 °C for 2 days. The identification of a single yeast colony was performed using DNA barcoding based on the internal transcribed spacer (ITS) sequence method with the primers ITS1 and ITS2 (Table 2). To validate the species of the isolated yeast, the ITS sequences were compared with those in the GenBank database (Accession number: 12683468) using the BLAST search program (https://www.ncbi.nlm.nih.gov/, accessed on 9 November 2018).

Table 2. Strains and plasmids used throughout the study.

Name	Relevant Description	References
Strains		
BY4741	S288C-derivative laboratory strain, MATa his3Δ1 leu2Δ0 met15Δ0 ura3Δ0	16
E. coli DH5 α	F-, φ80, lacZΔM15, Δ(lacZYA-argF) U169 endA1, recA1, hsdR17(rk-, mk+) supE44, λ-, thi-1, gyrA96, relA1, phoA	Takara Bio, Kyoto, Japan
BY4741△FDH1	*Saccharomyces cerevisiae* BY4741, △FDH1	This study
BYzm4741FDH1	BY4741△FDH1, zmFDH1	This study
plasmid		
Cas9	p414-TEF1p-Cas9-CYC1t, CEN6/ARSH4 origin, TRP1, TEF1p promoter, codon optimized Cas9 with C-terminal SV40 tag, AmpR	Addgene
gRNA	p426-SNR52p-gRNA.CAN1.Y-SUP4t, PSNR52-gRNA-SUP4TT	Addgene
sgRNA-gRNA	Ligation sgRNA into the gRNA scaffold of plasmid gRNA	This study
ZmFDH1-PYES2	Ligation zmFDH1 into the plasmid PYES2	This study

2.2. Growth Curve Measurements

Yeast was cultured with yeast extract–peptone–dextrose (YPD) medium containing 30% glucose (*w*/*v*) at 30 °C with shaking at 180 rpm for 12–16 h until the cell density reached 2 × 10^8 CFU/mL. An amount of 7% of the inoculation volume was added to YPD

medium containing 60% glucose or 2% glucose, respectively. In addition, the latter was used as control. Then, the yeast was cultured at 30 °C with shaking at 180 rpm, and the biomass of the yeast was assessed every 8 h, or the OD values were assessed every 6 h. The sample in logarithmic phase was used in the following experiment.

2.3. POD, SOD and CAT Enzyme Activities Determination

The culture solution at 24 h was centrifuged at 9000 rpm for 10 min at 4 °C, after which the yeast cells were washed with PBS 4 times and then suspended in PBS at a concentration of 2×10^9 CFU/mL. The enzyme activities of peroxidase (POD), superoxide dismutase (SOD) and catalase (CAT) were assayed according to the kit instructions of the POD activity assay kit (BC0090), SOD activity assay kit (BC0170) and CAT activity assay kit (BC0200), respectively (Beijing Solarbio Science & Technology Co., Ltd., Beijing, China).

2.4. Glycerol and Trehalose Content Determination

To create a standard curve for determining glycerol concentration, 0.0, 0.25, 1.0, 1.5 and 2.0 mL of glycerol at a concentration of 0.03 mg/mL were adjusted to 2 mL by adding sterile water, respectively, and then reacted with acetylacetone solution (1.2 mL) and acetylacetone solution (1.2 mL) in a 70 °C water bath for 1 min. The OD values of the mixture were detected at 410 nm [20]. The standard curve obtained was y = 19.282x + 0.0356 (R^2 = 0.991). The yeast that was cultured for 24 h was washed with sterile water 4 times and then centrifuged at 4 °C and 9000 rpm for 10 min. After freezing and thawing 3 times, the supernatant was used for the determination of glycerol.

To create a standard curve for determining trehalose content, 0.0, 0.5, 1.0, 2.0 and 3.0 mL of trehalose (1 g/L) were mixed with trichloroacetic acid (0.5 m, 4 mL) and were then adjusted to 25 mL by adding sterile water, respectively. Then, 1 mL of each sample was mixed with 5 mL of anthrone–sulfuric acid (2 g/L), and the mixture reacted in boiling water for 10 min. The OD values of the samples were detected at 410 nm [21]. The standard curve obtained was y = 6.2746x + 0.0442 (R^2 = 0.9993). Yeasts were treated with trichloroacetic acid (0.5 M) on ice for 1 h to extract intracellular trehalose and then centrifuged at 4 °C and 14,000 rpm for 10 min. After the supernatant was mixed with trichloroacetic acid (0.5 M), each sample was reacted with anthrone–sulfuric acid in boiling water for 10 min, and the solution was then used for the determination of trehalose content.

2.5. iTRAQ Experiment

The yeast suspensions were centrifuged at 9500 rpm for 10 min at 4 °C, and the yeast cells were washed with sterile water 3 times. Proteins were extracted using lysis buffer (8 M urea, 40 mM Tris-HCl, 2 mM EDTA and 10 mM DTT, pH 8.5) and magnetic beads (diameter 5 mm). After the mixture was put in a TissueLyser for 2 minutes at 50 Hz and then centrifugated with 25,000× *g* at 4 for 20 min, the supernatant was reduced with 10 mM dithiothreitol at 56 °C for 1 h and alkylated by 55 mM iodoacetamide for 20 min. The mixture was centrifugated, and the supernatant containing the proteins was obtained. After the extracted protein was digested with Trypsin Gold (Promega, Madison, WI, USA), peptides were desalted with a Strata X C18 column (Phenomenex, Torrance, CA, USA). Then, the peptides were dissolved in 30 μL 0.5 M TEAB and combined with the iTRAQ labeling reagents in the iTRAQ Reagent 8-plex Kit (Sigma Aldrich Inc., St. Louis, MI, USA).

The labelled peptides were separated with an LC-20AB HPLC Pump system, which was coupled with a high pH RP column (Shimadzu, Kyoto, Japan). Then, each fraction was separated using the UltiMate™ 3000 UHPLC system (Thermo Fisher Scientific, San Jose, CA, USA). The peptides separated from Nano HPLC were subjected to tandem mass spectrometry Q EXACTIVE HF X (Thermo Fisher Scientific, San Jose, CA, USA) for data-dependent acquisition (DDA) detection by Nano electrospray ionization. The iTRAQ data were analyzed using Mascot software (version 2.3.02, Matrix Science Inc., NEB, Ipswich, MA, USA). When the FC (fold change) of a protein is greater than 1.2 or less than 0.83, it is considered a DEP. Functional annotations of the DEPs were conducted using the Blast2GO

program against the nonredundant protein database (NR, NCBI). The Kyoto Encyclopedia of Genes and Genomes (KEGG) database and the COG database (NCBI) were used to classify and group the identified proteins.

2.6. Construction of the Mutant Strains

The engineered *S. cerevisiae* strains with a knocked-out *scFDH1* gene were constructed using the CRISPR/Cas9 method that was described in previous study [22,23]. The strains and plasmids used in the experiment were shown in Table 2. Plasmids p414-TEF1p-Cas9-CYC1t (#43802) and p426-SNR52p-gRNA.CAN1.Y-SUP4t (#43803) were obtained from Addgene Inc. The NGG locus was found, and sgRNA was created online (http://crispr.mit.edu/, accessed on 10 December 2021) based on the sequence of *scFDH1*. sgRNA was ligated into the gRNA scaffold of plasmid gRNA through Bfa I enzyme digestion to construct the gRNA expression vector sgRNA-gRNA.

S. cerevisiae BY4741 was employed as the host strain to inactivate the *scFDH1* gene. Total genomic DNA of BY4741 was used as a template to amplify the homology arms scFDH1-UP and scFDH1-Down, with primers scFDH1-up-F/scFDH1-up-R and scFDH1-down-F/scFDH1-down-R, respectively. The PCR product purification kit (Tiangen biochemical technology (Beijing) Co., Ltd., Beijing, China) was used to purify scFDH1-UP and scFDH1-Down fragments for fusion PCR amplification to create homology arms for repair. The fused fragments were then ligated into the pMD19-T vector and transformed to *Escherichia coli* DH5α competent cells. Primers M13-F and M13-R (Table 2) were used for the verification of the positive colony.

Repair homologous arms (10 pmol), plasmid Cas9m (3 μg) and sgRNA-gRNA (3 μg) were electrically transformed into approximately 5×10^5 BY4741 competent cells at 1500 KV. After being cultured at 30 °C for 3 h, the yeasts were spread on a YPD plate containing G418. The deletion of the scFDH1 gene was confirmed by PCR amplification with primers scFDH1-UP-F/scFDH1-DOWN-R and scFDH1-KpnI-F/scFDH1-BamHI-R. The PCR products were purified and ligated into the pMD19-T vector and then transformed to *E. coli* DH5α competent cells. The Primers M13-F and M13-R (Table 2) were used for the verification of the positive colony. The yeast mutants with the *scFDH1* gene knocked-out were named BY4741△scFDH1.

The *FDH1* gene from *Z. mellis* was amplified using primers zmFDH1-KpnI-F and zmFDH1-BamHI-R. The PCR product purification kit (Tiangen biochemical technology (Beijing) Co., Ltd., Beijing, China) was used to purify the amplified *zmFDH1*, which was then ligated into the pYES2 plasmid through *Kpn*I and *BamH*I double digestion to construct the plasmid zmFDH1-PYE2. The plasmid zmFDH1-PYE2 was transformed into *E. coli* DH5α competent cells and then grown on an LB plate containing ampicillin overnight at 37 °C. Primers T7 and CYC1 Terminator were used to identify positive colonies. The plasmid zmFDH1-pYES2 was transformed into the BY4741△scFDH1 cells and then spread on an SC-URA plate at 30 °C. Primers T7 and CYC1 terminator were used to confirm the positive clones. The confirmed yeast mutants, which contain the *zmFDH1* gene, were named BYzm4717FDH1.

2.7. ATP and NADH Content Determination

The yeast culture solution at 24 h was centrifuged at 9000 rpm and 4 °C for 10 min. The ATP content was assayed according to the kit instructions of the ATP content assay kit (BC0300) (Beijing Solarbio Science & Technology Co., Ltd., Beijing, China). After the extract solution was added, the yeasts were broken by an ultrasonic method for 1 min and then centrifugated at 9000 rpm and 4 °C for 10min. The supernatant was mixture with chloroform. After being centrifuged at 9000 rpm and 4 °C for 3 min, the supernatant was used for ATP content determination.

The NADH content was assayed according to the kit instructions of the NADH content assay kit (BC0310) (Beijing Solarbio Science & Technology Co., Ltd., Beijing, China). After the alkaline extract solution was added, the yeasts were broken by an ultrasonic method

for 1 min and boiled for 5 min. After being centrifuged at 9000 rpm and 4 °C for 3 min, the supernatant was added to an equal volume of acid extract solution. The mixture was centrifuged at 9000 rpm and 4 °C for 10 min, and the supernatant was used for NADH content determination.

2.8. qRT-PCR Amplification

The relative expression levels of *FDH1* in BY4741, BY4741△scFDH1 and BY4717zmFDH1 were measured using qRT-PCR. Total RNA was extracted using Trizol reagent (Invitrogen, Carlsbad, CA, USA). The PCR primers for the reaction were designed using primer premier 6.0 (Table 2). PCRs were performed with primers FDH1-F/FDH1-R using the Applied Biosystems 7500 Real-Time Fast Real-time PCR System (Life Technologies, Carlsbad, CA, USA). The comparative CT method ($2^{-\Delta\Delta CT}$) was used to determine the relative level of mRNA expression [24], and ACT was used as a housekeeping gene.

2.9. Data Analysis

All experiments were performed in triplicate, and the data are reported as the mean (n = 3, *biologically independent* replicates) ± standard error. Statistical *analyses* were performed by *one-way analysis of variance (ANOVA) followed by Tukey test* and two-way ANOVA using SPSS (IBM® SPSS® Statistics, versus 19.0), and differences of $p < 0.05$ were considered significant.

3. Results

3.1. Identification of Yeasts in Honey and the Influence of Sugar Stress on Yeast Growth

Yeasts were isolated from 18 honey samples (Table S2), mainly including winter honey, loquat honey and litchi honey. Among these samples, six (EH2, WH1, LQH1, LQH4, LCH5 and LCH6) had high yeast counts. DNA metabarcoding technology was used to identify the yeast community of these six samples, resulting in the identification of *Z. rouxii*, *Z. mellis* and *Z. siamensis*.

As shown in Figure S1, the growth of *Z. rouxii*, *Z. mellis* and *Z. siamensis* in 60% YPD was investigated. For *Z. mellis* and *Z. rouxii*, the biomass of the group cultured with 60% YPD had the same biomass as the controls at 56 h. For *Z. siamensis*, the biomass of the 60% YPD group was lower than that of the control. The controls showed a period of exponential growth before 24 h, while the 60% glucose YPD groups grew quickly between 16 and 40 h, indicating that growth is delayed in the hypertonic environment. Considering the growth rate and biomass, the yeasts that were cultured for 24 h were used for the following experiments. As a result, the contents of glycerol and trehalose in yeast under 60% glucose YPD increased, as well as the activity of the CAT, SOD and POD enzymes. The resistance of *Z. mellis* to high sugar stress was better than *Z. siamensis*, but weaker than *Z. rouxii*, as evidenced by the results of the growth situation, enzyme activity and glycerol and trehalose contents (Figure S1).

3.2. iTRAQ Data Analysis

The mechanism of sugar tolerance in *Z. mellis* was analyzed by proteomic techniques. The results showed that there were 522 DEPs in the 60% glucose YPD group compared with the 2% glucose YPD group, of which 303 (58.05%) were upregulated and 219 (41.95%) were downregulated (Table S3). Detailed information about the DEPs, including protein sequences and the values of SD, are listed in Table S4. According to the KOG functional categories, DEPs were classified into 23 groups. Among them, most DEPs were related to post-translational modification, protein turnover and chaperones (16.19%), amino acid transport and metabolism (15.19%), and energy production and conversion (14.85%). Additionally, formate dehydrogenase1 (FDH1), which catalyzes the decomposition of formic acid to produce CO_2 and the reduction of NAD+ to NADH, showed a great increase in response to high sugar stress [15]. The DEPs involved in the metabolic pathway of trehalose, glycerol and the TCA cycle, etc., are listed in Table 3. Among them, the proteins related

to trehalose and glycerol degradation were all downregulated, and most of the proteins related to the glycolysis and pentose phosphate pathways were also downregulated. In contrast, most proteins related to TCA and respiration were upregulated.

Table 3. Partial DEPs of *Z. mellis* in response to sugar stress.

Protein_ID	Description	60% Glucose Group vs. 2% Glucose Group
TCA cycle		
GCE97816.1	NAD-dependent isocitrate dehydrogenase	1.33
GCF00601.1	phosphoglycerate kinase	0.74
GCE97119.1	cytochrome b subunit of succinate dehydrogenase, Sdh3p	1.25
GCE99324.1	NADP-dependent isocitrate dehydrogenase	0.44
GCF01027.1	malate dehydrogenase, cytoplasmic	1.25
GCE98908.1	2-oxoglutarate dehydrogenase complex E2 component	1.28
GCE99351.1	citrate (Si)-synthase	1.29
GCF00374.1	succinate dehydrogenase complex, subunit B	1.58
GCE97219.1	succinate dehydrogenase assembly factor 2	0.79
GCF01476.1	membrane anchor subunit of succinate dehydrogenase, Sdh4	1.48
Glycolysis		
GCF00125.1	glucokinase	0.58
GCF00259.1	hexokinase A	0.64
GCE99269.1	fructose-bisphosphate aldolase 1	0.69
GCE98585.1	glyceraldehyde-3-phosphate dehydrogenase	1.33
GCE97503.1	glyceraldehyde-3-phosphate dehydrogenase 1	1.21
Pentose phosphate pathway		
GCF00070.1	enolase-phosphatase E1	0.55
GCE97493.1	ribulose-phosphate 3-epimerase	0.67
GCF01076.1	sedoheptulose-7-phosphate: D-glyceraldehyde-3-phosphate transaldolase	0.69
GCF01082.1	glucose-6-phosphate isomerase	0.78
GCE98569.1	triosephosphate isomerase	0.8
GCF01275.1	glucose-6-phosphate 1-dehydrogenase	1.25
GCF00672.1	ribose-5-phosphate isomerase rki1	1.55
Respiratory chain		
GCF00431.1	ubiquinol-cytochrome c reductase core subunit 10 qcr10	1.4
GCE98211.1	NADH: ubiquinone oxidoreductase	0.48
GCF01526.1	cytochrome c oxidase subunit 6	0.81
GCE97076.1	cytochrome c oxidase subunit 4	1.26
GCF00071.1	iso-1-cytochrome c	1.29
GCF01652.1	cytochrome c oxidase subunit 2	1.3
GCE99676.1	Cu-binding protein	1.31
Trehalose and glycerol degradation		
GCE99412.1	phosphoglucomutase-2	0.62
GCF00370.1	glycerol kinase	0.79
GCE99841.1	glycerol-3-phosphate/dihydroxyacetone	0.83
GCE98648.1	phosphate acyltransferase dihydroxyacetone kinase 1	0.72

Table 3. *Cont.*

Protein_ID	Description	60% Glucose Group vs. 2% Glucose Group
Antioxidant		
GCE98999.1	superoxide dismutase (Mn), mitochondrial	1.21
GCE99208.1	catalase T	2
Ergosterol synthesis		
GCE98125.1	phosphomevalonate kinase	0.64
GCE98064.1	diphosphomevalonate decarboxylase	0.68
GCE98950.1	phospholipid:diacylglycerol acyltransferase	0.77
GCF01680.1	squalene epoxidase	0.8
GCE99731.1	erg10, acetyl-CoA C-acetyltransferase	1.61
GCE99856.1	C-24(28) sterol reductase	1.49
GCE99284.1	RNA polymerase C-22 sterol desaturase	1.52
GCE97050.1	farnesyl pyrophosphate synthetase	0.66
Cell wall		
GCE99669.1	UDP-glucose-4-epimerase	0.48
GCE98182.1	UDP-*N*-acetylglucosamine pyrophosphorylase	0.73
GCE99673.1	chitin synthase, class 3	0.75
GCE99446.1	glutamine-fructose-6-phosphate transaminase	0.77
GCE99630.1	chitin synthase, class 1	0.82
GCE97781.1	Peroxin	0.75
NADH generation		
GCE97061.1	formate dehydrogenase 1	1.71
GCE97099.1	formate dehydrogenase 1	1.84
GCE98400.1	formate dehydrogenase 1	10

3.3. Construction of the Mutant Strains Y4741△scFDH1 and BYzm4717FDH1

The process of constructing *S. cerevisiae* BY4741 strains with different *FDH1* statuses is shown in Figure 1. The sgRNA sequence that was designed based on the sequence of the *scFDH1* gene was 5′–GTTACACAGAGCTTCAGGTT–3′. The expression vector was then constructed by ligating sgRNA into the gRNA scaffold of gRNA. Because *scFDH1* was knocked out, PCR amplification with the primers FDH1-Up-F and FDH1-Down-R yielded a PCR product of 2091 bp (Figure 1C2); however, PCR amplification with the primers FDH1-KpnI-F and FDH1-BamHI-R yielded no corresponding band (Figure 1C3). The positive clones were screened and named BY4741△scFDH1.

The *FDH1* gene was amplified from *Z. mellis* and ligated into the plasmid pYES2, and the product was transformed into the BY4741△scFDH1 strain. A 1068 bp band was observed through PCR amplification with the primers zmFDH1-KpnI-F and zmFDH1-BamHI-R, indicating that the yeast strain BYzmFDH1 containing the *zmFDH1* gene had been obtained (Figure 1C).

3.4. Effect of Sugar Stress on the Growth of BY4741△scFDH1 and BYzm4717FDH1

The OD values of BY4741, BY4741△scFDH1 and BYzm4717FDH1, which were grown in 20% and 60% glucose YPD for 3 d, respectively, were determined every 6 h (Figure 2A). The results revealed that there was no significant difference among these three strains in 20% glucose YPD at 24 h. The OD value of BY4741△scFDH1 was significantly reduced compared with BY4741 in 60% glucose YPD ($p < 0.01$) at 24 h, while BYmzFDH1 resumed its regular growth pattern, showing no difference from BY4741.

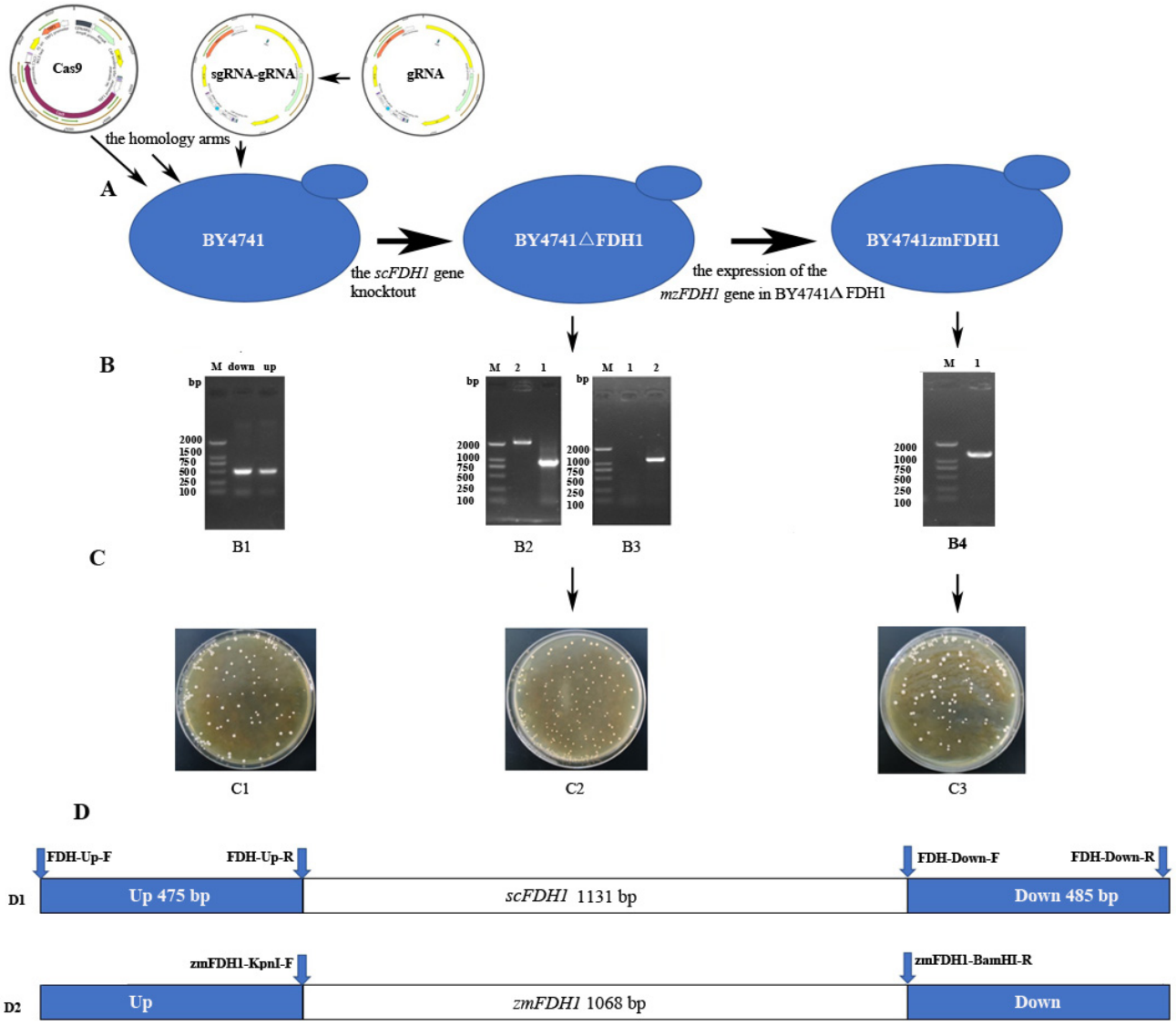

Figure 1. Strain construction. (**A**): Schematic of construction of BY4741△scFDH1 and BY4717mzFDH1 strains. (**B**): PCR amplification. (1) Product of the homology arms; M: maker; down: down repair homologous arm; up: up repair homologous arm. (2) Confirmation of BY4741△scFDH1 strain by PCR using primers FDH1-Up-F and FDH1-Down-R; M: marker; 1: negative colony; 2: positive colony. (3) Confirmation of BY4741△scFDH1 strain by PCR using primers FDH1-KpnI-F and H1-BamHI-R. (4) PCR result of BYmzFDH1 strain; M: marker; 1: negative colony; 2: positive colony. (**C**): Colonies of BY4741, BY4741△scFDH1 and BYmzFDH1 strains; M: marker; 1: negative colony. (**D**): The sites of the primers.

As shown in Figure 2B,C, the intracellular glycerol and trehalose contents in yeasts under high sugar stress were measured. Our results showed that glycerol and trehalose in *Z. mellis* accumulated in yeasts significantly during fermentation with 60% glucose YPD (Supplementary Figure S1). In comparison to BY4741, the amount of intracellular glycerol, as well as the activity of SOD, CAT and POD, decreased in BY4741△scFDH1, but the amount of intracellular glycerol and trehalose, as well as POD activity, increased in BYzm4717FDH1.

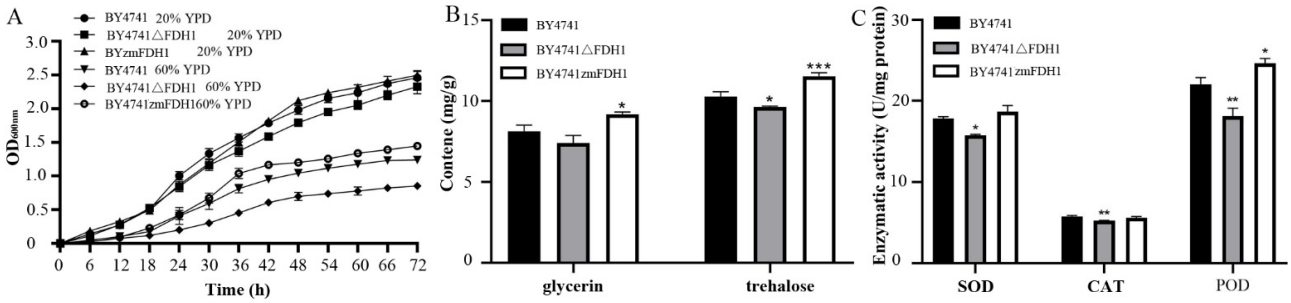

Figure 2. The influence of sugar stress on the growth of BY4741, BY4741△scFDH1 and BY4717zmFDH1. (**A**): The OD600 values of BY4741, BY4741△scFDH1 and BY4717zmFDH1. (**B**): The intracellular glycerol and trehalose contents of BY4741, BY4741△scFDH1 and BY4717zmFDH1 under 60% YPD. (**C**): The enzyme activities of CAT, SOD and POD of BY4741, BY4741△scFDH1 and BY4717zmFDH1 under 60% YPD. (**A**): Two-way analysis of variance (ANOVA); (**B**,**C**): one-way analysis of variance (ANOVA) followed by Tukey test. * represents significant difference, p value < 0.05, ** represents extremely significant difference between treatment and control, p value < 0.01, and *** represents extremely significant difference between treatment and control, p value < 0.001.

As shown in Figure 3, the relative expression of *FDH1* and the contents of ATP and NADH in yeasts were measured. The *FDH1* gene was almost not expressed in BY4741△scFDH1 but was expressed normally in BYzm4717FDH1, indicating that *FDH1* was successfully knocked out in BY4741△scFDH1 and expressed in BYzm4717FDH1. Compared with BY4741, the ATP and NADH contents decreased in BY4741△scFDH1, but there was no difference in BYzm4717FDH1, indicating that FDH1 has a significant effect on ATP and NADH synthesis.

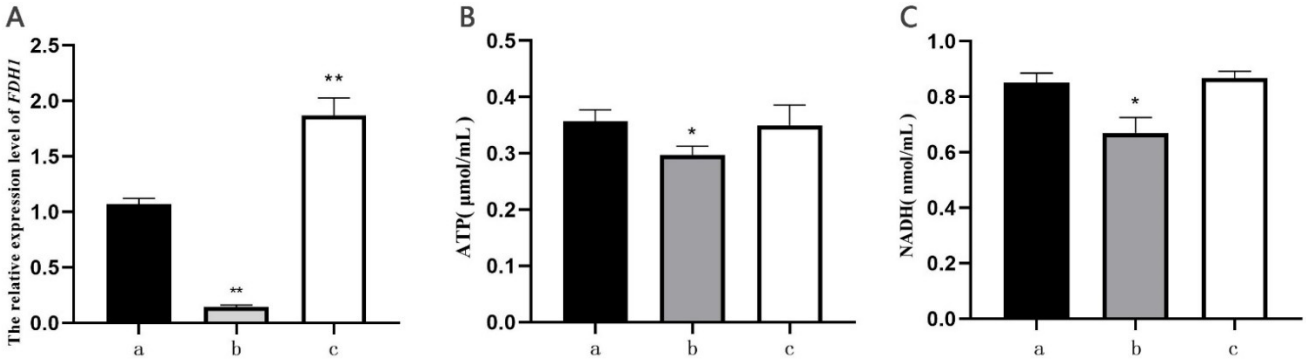

Figure 3. The influence of sugar stress on the relative expression of FDH1gene (**A**), ATP content (**B**) and NADH content (**C**) of BY4741, BY4741△scFDH1 and BY4717zmFDH1. a: BY4741, b: BY4741△scFDH1, c: BY4717zmFDH1 (one-way analysis of variance (ANOVA) followed by Tukey test). * represents significant difference, p value < 0.05, and ** represents extremely significant difference between treatment and control, p value < 0.01.

4. Discussion

Honey contains a large number of nutrients, including protein, amino acids, enzymes, minerals, vitamins and aromatic compounds except sugar. Honey also has antioxidant and antibacterial activity, which can be used for anti-aging and burn treatments [25]. In addition, honey is also a natural food to make wine using yeast. A few studies have shown that mixed yeast strains show better fermentation characteristics, such as increasing glycerol content and total acidity and producing a variety of volatile phenols, esters, ketones and other special substances [26]. In this study, *Z. mellis* that was isolated from honey showed high hypertonic tolerance in response to high sugar stress with the potential for food fermentation.

Hyperosmotic stress stimulates a large variety of adaptive responses in yeast cells that affect many different physiological functions to adapt to the environment. During the fermentation process, because high concentrations of sugar and accumulated ethanol have toxic effects on yeast cells, yeasts have a series of physiological regulatory mechanisms to resist high osmotic stress, leading to growth delays [27–29]. Previous studies have shown that yeast can produce and retain metabolically compatible osmolytes, including intracellular glycerol and trehalose, to adapt to the hyperosmotic environment [30–32]. Transcriptomics analysis revealed that some genes involved in the pathway of the high osmolarity glycerol mitogen-activated protein kinase (HOG-MAPK) signal transduction and trehalose synthesis, as well as the oxidative stress response, were upregulated under high-glucose tolerance in *Z. mellis* [6]. In addition, the morphological and structural properties of the cell wall and plasma membrane can also be regulated [33].

In this study, proteome analysis revealed that the proteins involved in the regulation of cell-wall, membrane and envelope biogenesis were all downregulated. Among them, Chitin cross-links with β-glucan to form a cell-wall skeleton and plays a key role in maintaining cell morphology and structure [34,35]. Ergosterol, an important component of the microbial cell membrane, can stabilize the membrane structure by combining with phospholipids to regulate membrane permeability, membrane fluidity, integrity and cell material transport [36]. Under alcohol treatment, the content of ergosterol in the cell membrane of *S. cerevisiae* can increase to inhibit membrane damage and maintain normal membrane permeability [36–38]. However, in this study, due to the growth delay, the proteins involved in cell-wall and ergosterol synthesis were downregulated.

Intracellular glycerol and trehalose, which can be used as osmotic protectants, will accumulate in yeast cells in response to external osmotic stress. It was reported that trehalose and glycerol can protect the cell membranes in response to sugar, NaCl and metal ions [7,39,40]. iTRAQ data revealed that the proteins involved in the degradation of glycerol and trehalose were downregulated in the assayed yeast. Among them, glycerol kinase, dihydroxyacetone kinase 1 and glycerol-3-phosphate/dihydroxyacetone phosphate acyltransferase (38) are involved in the degradation of glycerol [41–43], and phosphoglucomutase-2 is involved in the degradation of trehalose [40]. In yeasts, there are two well-established pathways to produce glycerol, including the Gcy-Dak pathway and the Gpd-Gpp pathway [7]. The proteins related to glycerol generation, including *TPS and otsB*, had been identified in response to high sugar stress in *Z. mellis* [6], but in this study, no proteins involved in these biosynthetic pathways were significantly differentially expressed. These results indicated that glycerol and trehalose also accumulated via decreased degradation, which is consistent with previous studies showing that glycerol accumulated under high osmotic pressure by retention [44]. As a result, this study revealed that osmotic protectants accumulated rapidly in the early stages of high-sugar fermentation to resist external hypertonic pressure in *Z. mellis*.

Many studies have shown that antioxidant enzymes, such as SOD, CAT and POD, can play an important role against reactive oxygen species (ROS) to protect organisms from oxidative damage [45–47]. When yeast is under stress, the intracellular ROS content will rapidly increase, and the enzyme activities and the expression level of the encoding genes will be upregulated to regulate the intracellular ROS balance [32,48]. SOD catalyzes two molecules of superoxide anion (O_2-) to generate hydrogen peroxide (H_2O_2) and oxygen (O_2), and CAT and POD then decompose H2O2 into H2O and O2 [49]. The improved antioxidant enzyme activities could enhance the high salt tolerance of *Z. rouxii* [32]. In addition, the expression level of SOD was upregulated, which was consistent with the result of transcriptomics analysis [6]. In *S. cerevisiae*, SOD could protect RNR from inactivation, and sod1Δ and sod2Δ mutants showed decreased growth under aerobic conditions [50]. In this study, the enzyme activities and protein expression of SOD, CAT and POD were increased during fermentation to eliminate the damaging effect of H_2O_2 on cells and avoid oxidative damage in a high-sugar environment.

Osmotic stress can increase the activities of MDH and SDH, which are the key enzymes of glucose metabolism and the TCA cycle and are involved in energy metabolism processes and respiration [51]. In fungi, the inhibition of enzyme activities involved in energy metabolism and respiration, especially SDH and MDH, resulted in the inhibition of mycelial growth [52]. Mitochondrial defects lead to the hyperaccumulation of ROS in response to salt stress [53].

In the proteome experiment, 45 proteins were identified that are related to energy metabolism, 29 of which were upregulated, while the other 16 were downregulated (Table S4). Among them, cytochrome c oxidase is the terminal enzyme of the mitochondrial membrane respiratory chain, and its function is directly related to ATP synthesis and associated with programmed cell death in yeast [54]. In addition, 7 of 10 proteins involved in the TCA cycle were upregulated (Table 2). Among these proteins, the expression levels of the SDH and MDH proteins were upregulated, which was consistent with the observed changes in enzyme activity. It has been shown that the expression of energy-related genes, especially those related to respiration and energy metabolism, increases with the duration of hyperosmolar stress in *S. cerevisiae* [55]. Upregulation of proteins in the respiratory chain and the TCA cycle can produce more ATP, providing energy for cells to adapt to hypertonic environments.

The protein with the greatest difference in expression was FDH1, which can oxidize formic acid to CO_2 and reduce NAD+ to NADH; it has been used in studies of coenzyme regeneration [19,56] and was upregulated under stress conditions [57,58]. NADH enters the electron transport chain through the glycerophosphate shuttle and malate aspartate acid shuttle, and acts as a respiratory substrate for ATP generation through oxidative phosphorylation. The overexpression of the *FDH* gene could increase the content of NADH and lead to a significant increase in intracellular ATP [59,60]. The increase in ATP had a significant inhibitory effect on the glycolysis pathway [61], and the proteome data also demonstrated a decrease in the expression of proteins involved in the glycolysis pathway. In this study, the knockout of the *FDH1* gene in *S. cerevisiae* slowed growth, lowered ATP, NADH, trehalose and glycerol contents, and decreased the enzyme activities of CAT, SOD and POD. However, the expression of the *zmFDH1* gene in the BY4741scFDH1 strain resulted in the resumption of growth, an increase in trehalose and glycerol contents, and an increase in the activity of the CAT, SOD and POD enzymes, suggesting that the *FDH1* gene may impact yeast hypertonic tolerance.

5. Conclusions

In this study, DNA metabarcoding technology was used to identify yeast species in honey. As a result, *Z. rouxii*, *Z. mellis* and *Z. siamensis* were identified. In the presence of a high sugar content (60%, *w*/*v*), yeast growth was delayed. In order to adapt to the hyperosmotic environment, *Z. mellis* increased the content of trehalose and glycerin and enhanced energy metabolism before other physiological adjustments. iTRAQ data showed that most of the proteins associated with cell growth, including the cell membrane, cell-wall synthesis and glycolysis and pentose phosphate pathways, etc., were downregulated in *Z. mellis*. Moreover, CRISPR/Cas9 technology constructed an *FDH1*-inactivated yeast, demonstrating that the *FDH1* gene has a significant effect on the yeast's hypertonic tolerance.

Supplementary Materials: The following supporting information can be downloaded at: https://www.mdpi.com/article/10.3390/pr10061193/s1, Figure S1. The influence of sugar stress on the growth of *Z. mellis*, *Z. rouxii* and *Z. siamensis*. Table S1. Honey samples from different botanical and geographical origins. Table S2. Number of isolated yeasts from honey samples. Table S3. DEPs of *Z. mellis* in response to sugar stress. Table S4. DEPs annotation.

Author Contributions: X.X. conceived and designed this research, analyzed the data and wrote the paper; Y.Z., Y.L., X.C. and H.Z. performed experiments and analyzed the data; Y.Z., W.Y. and X.X. designed the experiments and edited the manuscript. All authors have read and agreed to the published version of the manuscript.

Funding: This research was funded by "The Natural Science Foundation of the Fujian Province, No.2020J01131023" (Fujian Provincial Department of Science and Technology).

Institutional Review Board Statement: Not applicable.

Informed Consent Statement: Not applicable.

Data Availability Statement: The data presented in this study are available in Table 3, Supplementary Tables S1–S4.

Conflicts of Interest: The authors declare no conflict of interest.

References

1. Mateo, R.; Bosch-Reig, F. Sugar profiles of Spanish unifloral honeys. *Food Chem.* **1997**, *60*, 33–41. [CrossRef]
2. Rawsthorne, H.; Phister, T.G. A real-time PCR assay for the enumeration and detection of *Zygosaccharomyces bailii* from wine and fruit juices. *Int. J. Food Microbiol.* **2006**, *112*, 1–7. [CrossRef] [PubMed]
3. Carvalho, C.M.; Meirinho, S.; Estevinho, M.L.F.; Choupina, A. Yeast species associated with honey: Different identification methods. *Arch. Zootec.* **2010**, *59*, 103–113. [CrossRef]
4. Liu, G.; Tao, C.; Zhu, B.; Bai, W.; Zhang, L.; Wang, Z.; Liang, X. Identification of *Zygosaccharomyces mellis* strains in stored honey and their stress tolerance. *Food Sci. Biotechnol.* **2016**, *25*, 1645–1650. [CrossRef] [PubMed]
5. Wrent, P.; Rivas, E.M.; Peinado, J.M.; de Silóniz, M.I. Strain typing of Zygosaccharomyces yeast species using a single molecular method based on polymorphism of the intergenic spacer region (IGS). *Int. J. Food Microbiol.* **2010**, *142*, 89–96. [CrossRef]
6. Liu, G.; Bi, X.; Tao, C.; Fei, Y.; Gao, S.; Liang, J.; Bai, W. Comparative transcriptomics analysis of *Zygosaccharomyces mellis* under high-glucose stress. *Food Sci. Hum. Wellness* **2021**, *10*, 54–62. [CrossRef]
7. Dakal, T.C.; Solieri, L.; Giudici, P. Adaptive response and tolerance to sugar and salt stress in the food yeast *Zygosaccharomyces rouxii*. *Int. J. Food Microbiol.* **2014**, *185*, 140–157. [CrossRef]
8. Giardina, B.J.; Stanley, B.A.; Chiang, H.L. Comparative proteomic analysis of transition of *Saccharomyces cerevisiae* from glucose-deficient medium to glucose-rich medium. *Proteome Sci.* **2012**, *10*, 40. [CrossRef]
9. Estéfani, G.R.; Amparo, Q.; José Manuel, G. iTRAQ-based proteome profiling of *saccharomyces cerevisiae* and cryotolerant species *S. uvarum* and *S. kudriavzevii* during low-temperature wine fermentation. *J. Proteomics.* **2016**, *146*, 70–79. [CrossRef]
10. Saini, P.; Beniwal, A.; Kokkiligadda, A.; Vij, S. Response and tolerance of yeast to changing environmental stress during ethanol fermentation. *Process Biochem.* **2018**, *72*, 1–12. [CrossRef]
11. Li, C.; Xu, Y.; Jiang, W.; Lv, X.; Dong, X. Effect of sodium chloride and cadmium on the growth, oxidative stress and antioxidant enzyme activities of *Zygosaccharomyces rouxii*. *J. Ocean Univ. China* **2014**, *13*, 460–466. [CrossRef]
12. Saito, H.; Tatebayashi, K. Regulation of the osmoregulatory HOG MAPK cascade in yeast. *J. Biochem.* **2004**, *136*, 267–272. [CrossRef]
13. Babazadeh, R.; Furukawa, T.; Hohmann, S.; Furukawa, K. Rewiring yeast osmostress signalling through the MAPK network reveals essential and non-essential roles of Hog1 in osmoadaptation. *Sci. Rep.* **2014**, *4*, 1–7. [CrossRef] [PubMed]
14. Guo, H.; Niu, C.; Liu, B.; Wei, J.P.; Wang, H.X.; Yuan, Y.H.; Yue, T.L. Protein abundance changes of *Zygosaccharomyces rouxii* in different sugar concentrations. *Int. J. Food Microbiol.* **2016**, *233*, 44–51. [CrossRef] [PubMed]
15. Noti, O.; Vaudano, E.; Giuffrida, M.G.; Lamberti, C.; Cavallarin, L.; Garcia-Moruno, E.; Pessione, E. Enhanced arginine biosynthesis and lower proteolytic profile as indicators of, *Saccharomyces cerevisiae*, stress in stationary phase during fermentation of high sugar grape must: A proteomic evidence. *Food Res. Int.* **2018**, *105*, 1011–1018. [CrossRef] [PubMed]
16. Tedersoo, L.; Anslan, S.; Bahram, M.; Põlme, S.; Riit, T.; Liiv, I.; Kõljalg, U.; Kisand, V.; Nilsson, R.H.; Hildebrand, F.; et al. Shotgun metagenomes and multiple primer pair-barcode combinations of amplicons reveal biases in metabarcoding analyses of fungi. *MycoKeys* **2015**, *10*, 1–43. [CrossRef]
17. Blaalid, R.; Kumar, S.; Nilsson, R.H.; Abarenkov, K.; Kirk, P.M.; Kauserud, H. ITS1 versus ITS2 as DNA metabarcodes for fungi. Mol. *Mol. Ecol. Res.* **2013**, *13*, 218–224. [CrossRef]
18. Pompanon, F.; Coissac, E.; Taberlet, P. Metabarcoding, a new way of analysing biodiversity. *Biofutur* **2011**, *319*, 30–32.
19. Magoč, T.; Salzberg, S.L. FLASH: Fast length adjustment of short reads to improve genome assemblies. *Bioinformatics* **2011**, *27*, 2957–2963. [CrossRef]
20. Bondioli, P.; Della, B.L. An alternative spectrophotometric method for the determination of free glycerol in biodiesel. *Eur. J. Lipid Sci. Technol.* **2005**, *107*, 153–157. [CrossRef]
21. Wang, X.H.; Zhang, Y.Y.; Wang, C.; Wang, C.L.; Hou, L. Intracellular level of trehalose in soy sauce yeasts under different stresses. *IERI Procedia* **2013**, *5*, 321–326. [CrossRef]
22. DiCarlo, J.E.; Norville, J.E.; Mali, P.; Rios, X.; Aach, J.; Church, G.M. Genome engineering in *Saccharomyces cerevisiae* using CRISPR-Cas systems. *Nucleic Acids Res.* **2013**, *41*, 4336–4343. [CrossRef] [PubMed]
23. Stovicek, V.; Borodina, I.; Forster, J. CRISPR-Cas system enables fast and simple genome editing of industrial *Saccharomyces cerevisiae* strains. *Metab. Eng. Commun.* **2015**, *2*, 13–22. [CrossRef] [PubMed]
24. Livak, K.J.; Schmittgen, T.D. Analysis of Relative Gene Expression Data using Real-Time Quantitative PCR. *Methods* **2002**, *25*, 402–408. [CrossRef] [PubMed]

25. Stagos, D.; Soulitsiotis, N.; Tsadila, C.; Papaeconomou, S.; Arvanitis, C.; Ntontos, A.; Karkanta, F.; Adamou-Androulaki, S.; Petrotos, K.; Spandidos, D.A.; et al. Antibacterial and antioxidant activity of different types of honey derivedfrom Mount Olympus in Greece. *Int. J. Mol.* **2018**, *42*, 726–734. [CrossRef]
26. Multari, S.; Guzzon, R.; Caruso, M.; Licciardello, C.; Martens, S. Alcoholic fermentation of citrus flavedo and albedo with pure and mixed yeast strains: Physicochemical characteristics and phytochemical profiles. *LWT* **2021**, *144*, 111133. [CrossRef]
27. Benjaphokee, S.; Hasegawa, D.; Yokota, D.; Asvarak, T.; Auesukaree, C.; Sugiyama, M.; Kaneko, Y.; Boonchird, C.; Harashima, S. Highly efficient bioethanol production by a *saccharomyces cerevisiae* strain with multiple stress tolerance to high temperature, acid and ethanol. *New Biotechnol.* **2012**, *29*, 379–386. [CrossRef]
28. Matallana, E.; Aranda, A. Biotechnological impact of stress response on wine yeast. *Lett. Appl. Microbiol.* **2017**, *64*, 103–110. [CrossRef]
29. Auesukaree, C. Molecular mechanisms of the yeast adaptive response and tolerance to stresses encountered during ethanol fermentation. *J. Biosci. Bioeng.* **2017**, *124*, 133–142. [CrossRef]
30. Noti, O.; Vaudano, E.; Pessione, E.; Garcia-Moruno, E. Short-term response of different *Saccharomyces cerevisiae* strains to hyperosmotic stress caused by inoculation in grape must: RT-qPCR study and metabolite analysis. *Food Microbiol.* **2015**, *52*, 49–58. [CrossRef]
31. Petelenz-Kurdziel, E.; Kuehn, C.; Nordlander, B.; Klein, D.; Klipp, E. Quantitative analysis of glycerol accumulation, glycolysis and growth under osmotic stress. *PLoS Comput. Biol.* **2013**, *9*, e1003084. [CrossRef] [PubMed]
32. Li, L.L.; Ye, Y.R.; Pan, L.; Zhu, Y.; Zheng, S.P.; Lin, Y. The induction of trehalose and glycerol in *Saccharomyces cerevisiae* in response to various stresses. *Biochem. Biophys. Res. Commun.* **2009**, *387*, 778–783. [CrossRef] [PubMed]
33. Willaert, R.G. The growth behavior of the model eukaryotic yeast *Saccharomyces cerevisiae* in microgravity. *Curr. Biotechnol.* **2013**, *2*, 226–234. [CrossRef]
34. Hartland, R.P.; Vermeulen, C.A.; Sietsma, J.H.; Wessels, J.G.H.; Klis, F.M. The linkage of (1–3)-β-glucan to chitin during cell wall assembly in *Saccharomyces cerevisiae*. *Yeast* **1994**, *10*, 1591–1599. [CrossRef]
35. Grün, C.H.; Hochstenbach, F.; Humbel, B.M.; Verkleij, A.J.; Sietsma, J.H.; Klis, F.M.; Kamerling, J.P.; Vliegenthart, J.F.G. The structure of cell wall α-glucan from fission yeast. *Glycobiology* **2005**, *15*, 245–257. [CrossRef]
36. Vanegas, J.M.; Contreras, M.F.; Faller, R.; Longo, M.L. Role of unsaturated lipid and ergosterol in ethanol tolerance of model yeast biomembranes. *Biophys. J.* **2012**, *102*, 507–516. [CrossRef]
37. Shobayashi, M.; Mitsueda, S.I.; Ago, M.; Fujii, T.; Iwashita, K.; Iefuji, H. Effects of culture conditions on ergosterol biosynthesis by *Saccharomyces cerevisiae*. *Biosci. Biotechnol. Biochem.* **2005**, *69*, 2381–2388. [CrossRef]
38. Henderson, C.M.; Block, D.E. Examining the role of membrane lipid composition in determining the ethanol tolerance of *Saccharomyces cerevisiae*. *Appl. Environ. Microbiol.* **2014**, *80*, 2966–2972. [CrossRef]
39. Mahmud, S.A.; Nagahisa, K.; Hirasawa, T.; Yoshikawa, K.; Ashitani, K.; Shimizu, H. Effect of trehalose accumulation on response to saline stress in *Saccharomyces cerevisiae*. *Yeast* **2009**, *26*, 17–30. [CrossRef]
40. Yoshiyama, Y.; Tanaka, K.; Yoshiyama, K.; Hibi, M.; Ogawa, J.; Shima, J. Trehalose accumulation enhances tolerance of *Saccharomyces cerevisiae* to acetic acid. *J. Biosci. Bioeng.* **2015**, *119*, 172–175. [CrossRef]
41. Terrazas, W.D.M.; Aizemberg, R.; Gattas, E.A.D.L. Using Pichia pastoris to produce recombinant glycerol kinase. *Rev. Cienc. Farm. Basica Apl.* **2014**, *35*, 279–284.
42. Wang, Z.X.; Kayingo, G.; Blomberg, A.; Prior, B.A. Cloning, sequencing and characterization of a gene encoding dihydroxyacetone kinase from *Zygosaccharomyces rouxii* NRRL2547. *Yeast* **2002**, *19*, 1447–1458. [CrossRef] [PubMed]
43. Zufferey, R.; Mamoun, C.B. The initial step of glycerolipid metabolism in Leishmania major promastigotes involves a single glycerol-3-phosphate acyltransferase enzyme important for the synthesis of triacylglycerol but not essential for virulence. *Mol. Microbiol.* **2005**, *56*, 800–810. [CrossRef] [PubMed]
44. Myers, D.K.; Lawlor, D.T.; Attfield, P.V. Influence of invertase activity and glycerol synthesis and retention on fermentation of media with a high sugar concentration by *Saccharomyces cerevisiae*. *Appl. Environ. Microbiol.* **1997**, *63*, 145–150. [CrossRef]
45. Chen, G.Q.; Ren, L.; Zhang, J.; Reed, B.M.; Zhang, D.; Shen, X.H. Cryopreservation affects ROS-induced oxidative stress and antioxidant response in Arabidopsis seedlings. *Cryobiology* **2015**, *70*, 38–47. [CrossRef]
46. Anjum, S.A.; Tanveer, M.; Hussain, S.; Shahzad, B.; Ashraf, U.; Fahad, S.; Tung, S.A. Osmoregulation and antioxidant production in maize under combined cadmium and arsenic stress. *Environ. Sci. Pollut. Res.* **2016**, *23*, 11864–11875. [CrossRef]
47. Ferrareze, J.P.; Fugate, K.K.; Bolton, M.D.; Deckard, E.L.; Campbell, L.G.; Finger, F.L. Jasmonic acid does not increase oxidative defense mechanisms or common defense-related enzymes in postharvest sugarbeet roots. *Postharvest Biol. Technol.* **2013**, *77*, 11–18. [CrossRef]
48. Lu, F.P.; Wang, Y.; Bai, D.Q.; Du, L.X. Adaptive response of *Saccharomyces cerevisiae* to hyperosmotic and oxidative stress. *Process Biochem.* **2005**, *40*, 3614–3618. [CrossRef]
49. Sahu, S.; Das, P.; Ray, M.; Sabat, S.C. Osmolyte modulated enhanced rice leaf catalase activity under salt-stress. *Adv. Biosci. Biotechnol.* **2010**, *1*, 39–46. [CrossRef]
50. Das, A.B.; Sadowska-Bartosz, I.; Königstorfer, A.; Kettle, A.J.; Winterbourn, C.C. Superoxide dismutase protects ribonucleotide reductase from inactivation in yeast. *Free Radic. Biol. Med.* **2018**, *116*, 114–122. [CrossRef]
51. Baroowa, B.; Gogoi, N. The effect of osmotic stress on anti-oxidative capacity of black gram (*Vigna Mungo* L.). *Exp. Agric.* **2017**, *53*, 84–99. [CrossRef]

52. Haghdoost, N.S.; Salehi, T.Z.; Khosravi, A.; Sharifzadeh, A. Antifungal activity and influence of propolis against germ tube formation as a critical virulence attribute by clinical isolates of *Candida albicans*. *J. Mycol Med.* **2016**, *26*, 298–305. [CrossRef] [PubMed]
53. Ludovico, P.; Rodrigues, F.; Almeida, A.; Silva, M.T.; Barrientos, A.; Côrte-Real, M. Cytochrome c release and mitochondria involvement in programmed cell death induced by acetic acid in *Saccharomyces cerevisiae*. *Mol. Biol. Cell.* **2002**, *13*, 2598–2606. [CrossRef] [PubMed]
54. Yale, J.; Bohnert, H.J. Transcript expression in *Saccharomyces cerevisiae*, at high salinity. *J. Biol. Chem.* **2001**, *276*, 15996–16007. [CrossRef]
55. Tishkov, V.I.; Popov, V.O. Protein engineering of formate dehydrogenase. *Biomol. Eng.* **2006**, *23*, 89–110. [CrossRef]
56. Suzuki, K.; Itai, R.; Suzuki, K.; Nakanishi, H.; Nishizawa, N.K.; Yoshimura, E.; Mori, Y.S. Formate dehydrogenase, an enzyme of anaerobic metabolism, is induced by iron deficiency in barley roots. *Plant Physiol.* **1998**, *116*, 725–732. [CrossRef]
57. Hourton-Cabassa, C.; Ambard-Bretteville, F.; Moreau, F.; Davy de Virville, J.; Rémy, R.; Francs-Small, C.C. Stress Induction of Mitochondrial Formate Dehydrogenase in Potato Leaves. *Plant Physiol.* **1998**, *116*, 627–635. [CrossRef]
58. Chen, Y.; Cai, R. Study and analytical application of inhibitory effect of captopril on multienzyme redox system. *Talanta* **2003**, *61*, 855–861. [CrossRef]
59. Berríos-Rivera, S.J.; Bennett, G.N.; San, K.Y. Metabolic engineering of *Escherichia coli*: Increase of NADH availability by overexpressing an NAD(+)-dependent formate dehydrogenase. *Metab. Eng.* **2002**, *4*, 217–229. [CrossRef]
60. Du, C.; Li, Y.; Xiang, R.; Yuan, W. Formate dehydrogenase improves the resistance to formic acid and acetic acid simultaneously in *Saccharomyces cerevisiae*. *Int. J. Mol. Sci.* **2022**, *23*, 3406. [CrossRef]
61. Liu, L.M.; Li, Y.; Shi, Z.P.; Du, G.C.; Chen, J. Enhancement of pyruvate productivity in torulopsis glabrata: Increase of NAD+ availability. *J. Biotechnol.* **2006**, *126*, 173–185. [CrossRef] [PubMed]